Vol 3 (3) (2022)

Measurement, Control, and Automation

Website: https:// mca-journal.org

ISSN 1859-0551

Applying image processing technology for Automatic mobile robot tracking and following steel weld seams

Huu Hoang Bui[1], Van Hieu Dang[1], The Truong Nguyen[1], Kim Anh Nguyen[1*], Khanh Quang Nguyen[1], Van Quang Binh Ngo[2]

[1] *The University of Danang – University of Science and Technology, 54 Nguyen Luong Bang, Danang 50000, Vietnam*
[2]*Faculty of Physics, University of Education, Hue University, Thua Thien Hue 49000, Vietnam*
[*]*Corresponding author E-mail: nkanh@dut.udn.vn*

Abstract

In order to inspect steel weld seams, most of the buildings, steel pillars, pipelines, storage tanks, etc. are currently still used in a manual manner. More specifically, technicians often use scaffolding systems for moving and carrying defect testing equipment. At this time, the job requires them to work in dangerous altitude conditions, even in environments containing harmful gases. Therefore, this paper will focus on developing a mobile robot to replace human in the work of carrying welding defect equipment. This helps to ensure worker safety, increase productivity and save costs. A computer vision is integrated into the robot to create a unified system to help see things around it and think by itself. The robot uses computer vision to automatically identify steel weld seam and align the movement direction to follow the welding seam. In addition, with a special design using a permanent magnet wheel system, the robot has the ability to move flexibly on the surface of large steel structures with a flexible tilt angle from 0˚ to 180˚.

Keywords: *Mobile robot, image processing technology, edge detection, sliding window, metal welding*

Symbols

Symbols	Units	Description
V_l, V_r	m/s	the left, right wheel speed
ω	rad/s	the angular velocity
m	kg	the weight of the robot
g	m/s^2	gravitational acceleration
K		the frictional coefficient
D	m	the swing arm
R	m	the distance between the wheels to the ICC
l	m	the distance between the centers of the wheels

Tóm tắt

Hiện nay, hầu hết công việc kiểm tra chất lượng mối hàn trong ngành công nghiệp chế tạo thiết bị, cấu kiện sắt thép như đóng tàu, trụ thép, đường ống dẫn, bồn, bể chứa,… vẫn được tiến hành theo phương thức thủ công. Để di chuyển và mang vác thiết bị kiểm tra khuyết tật, người ta phải sử dụng đến hệ thống dàn giáo. Lúc này, công việc yêu cầu kỹ thuật viên phải làm việc trong điều kiện có độ cao nguy hiểm cao, thậm chí trong môi trường chứa khí độc hại. Chính vì vậy, nghiên cứu này sẽ tập trung trên việc thiết kế và chế tạo thực nghiệm robot tự hành để thay thế cho con người để thực hiện các công việc mang vác thiết bị kiểm tra khuyết tật đường hàn. Công việc này giúp đảm bảo an toàn lao động, tăng năng suất và giảm thiểu chi phí.
Nghiên cứu ứng dụng thị giác máy tính giúp robot tự động nhận diện đường hàn và căn chỉnh hướng di chuyển để bám theo đường hàn. Ngoài ra, với thiết kế dẫn động đặc biệt dùng hệ bánh xe nam châm vĩnh cửu giúp robot có khả năng di chuyển linh hoạt trên bề mặt của cấu kiện thép có kích thước lớn với góc nghiêng thay đổi linh hoạt từ 0˚ đến 180˚.

1. Introduction

In the manufacturing industries including shipbuilding, welds are often subjected to great pressure and exposed to highly corrosive seawater, so weld quality requirements are very important. Therefore, weld inspection must be performed strictly before the products are put into use [1]. However, nowadays, most workers still inspect welds manually. Workers often have to work in high-risk environmental conditions (on the hull of a ship with several tens of meters high, even when the ships are on the sea) causing unsafety at work, a direct danger to workers performing the work. Due to the large workload and unfavorable working environment, errors during weld inspection may still occur, and the quality of work is affected by objective factors [2]. Therefore, the design of a self-propelled robot that completely replaces humans to perform welding inspection work will bring a lot of practical significance. This design will help improve the cost-effectiveness of testing, as well as reduce the risk to human resources. The robot can operate continuously for many hours without being affected by the weather. This enhances performance and meets requirements in large projects. This field also poses challenges for domestic and foreign researchers. The automatic robot research project with image processing technology also promotes the research process of students, applying modern technology to the industrial production industry.

Received: 9 July 2022; Accepted: 8 December 2022.

In 2012, the first vertical surface grabbing robot studied to measure radioactive storage tanks with a robot weight of about 3 kg was introduced [3]. By 2018, a new study about low-cost wall climbing robot still relying on the vacuum machine method to increase adhesion on surfaces was published and the robot payload was only 500 g [4]

In 2011, the robot stuck to the steel surface based on the attraction of the electromagnet, was introduced in [5]. These studies are interesting because they can be changed at will. Later, robotics studies using permanent magnets were also carried out as on [6] and [7]. The main advantage of the permanent magnet wheels is that no energy is wasted on adhesion, instead choosing a motor with large torque to deal with the friction force, which also interferes with the robot control. This study focuses on image processing technology to identify and control the robot to follow the welding seam. The characteristic of the metal welding is that it always leans on the metal surface a joint in the shape of fish scales or water beads [8]. Based on this shape characteristic along with the color, the sharpness of the welding and applying image processing methods as on [9], the robot can detect the fish scale lines of the welding [10], calculate the deflection angle to adjust the correct direction and follow to the actual welding seam. With the metal flat surface, it is too difficult to detect welding by color. By the different threshold color between surface and welding, algorithm image processing can detect this [11]. The robot is capable of carrying detectors and other supporting devices that help in performing welding fault-checking work.

Specifically, this paper proposes to design an automatic robot moving along the metal welding seam, using a permanent magnet wheel. The robot moves on four wheels controlled by the differential transmission [12]. Using a computer vision system to detect the welds, it is possible to calculate deviations to help the robot align in the right direction. The feature of saving image data and allowing remote monitoring access is also mentioned [13]. In addition, the robot can operate in automatic and manual modes. In manual control mode, technicians use hand-held devices to directly control the robot when there is a problem without determining the path to move or the operator wants to control the robot at his own discretion.

The rest of this paper is organized as follows. Section 2 presents robot components, including: image processing module; calculate the traction force and torque of the drive motors to help the robot move on the steel surface with an unrestricted angle of inclination, and finally the control method for the robot to automatically follow the welding line. Experimental results and evaluations are made in Section 3 and general conclusions are presented in Section 4.

2. Building the construction of robot

2.1. Image pre-processing

In this section, the study deals with the welding seam detection process using image processing algorithms. However, the problem arises: the commonly used method is color detection to distinguish the object from the surrounding environment But there are many difficulties in this topic because the color of the welding seam and the metal surface are almost duplicate. Based on the properties of the welding, whether a qualified or unqualified welding seam which is left on the metal surface is a fish scale weld or an elongated water particle shape. Using the geometry as well as the sharpness of the welding seam, the research has combined two main image processing methods, edge detection method and sliding window protocol, to apply them to the fabrication of weld tracking robots.

- Edge Detection Method: In the image, there are often components such as smooth areas, edges, and noise. Therefore, Canny algorithm is one of the most important algorithms used to detect edges in images.
- Sliding Window Protocol: Using a loop that draws sliding windows along the frame, locates the white pixels in each window frame, determining the average x coordinate of those pixels. Each average position x is used as the x coordinate in the (x, y) coordinate system and based on that to reconstruct the welding seam.

Based on two main methods above, the study proposes the principle introduced in [13], [14] and designs the block diagram of the welding seam determination algorithm, as in Figure 1.

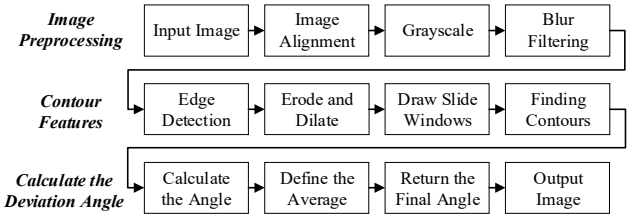

Figure 1: Image processing steps

2.1.1. *Pretreatment*

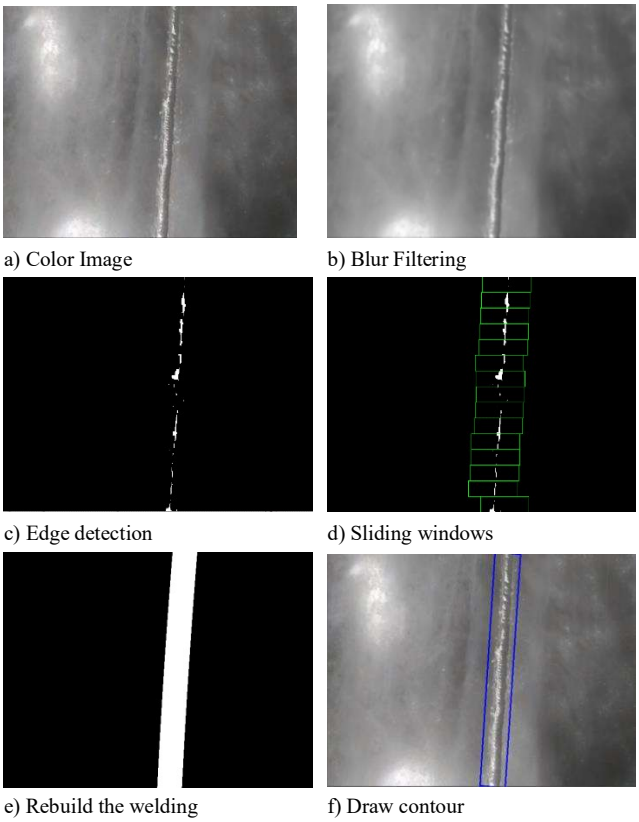

Figure 2: Results of the image processing

The input image is extracted from the camera as in Figure 2.a consisting of three colour channels: red, green, blue is converted to a gray image consisting of only one colour channel (from three matrices to one matrix) to reduce processing and calculation time.
The gray image is then filtered through a blur filter to remove noise. Aligning the image to the front view helps to reduce the error when calculating the offset angle in Figure 2.b.

2.1.2. *Finding contours*

The edge detection algorithm will use the image results from the preprocessing step to determine the edge of the welding using the Canny algorithm. The Canny algorithm will execute four main steps: noise reduction, finding image gradient intensity, non-maximum suppression and threshold filtering [10]. The gradient value of each pixel is calculated based on the derived image G_x and G_y, as in Eq. (1):

$$Edge - Gradient = \sqrt{G_x^2 + G_y^2} \quad (1)$$

The gradient value of each pixel will be compared with the threshold to decide whether to keep it or not. The result is as Figure 2.c.
Using the edges of the welding to find white pixels and rebuild the welding by the sliding window protocol with the algorithm diagram in Figure 3. The result of the sliding window algorithm is as shown in Figure 2.d.

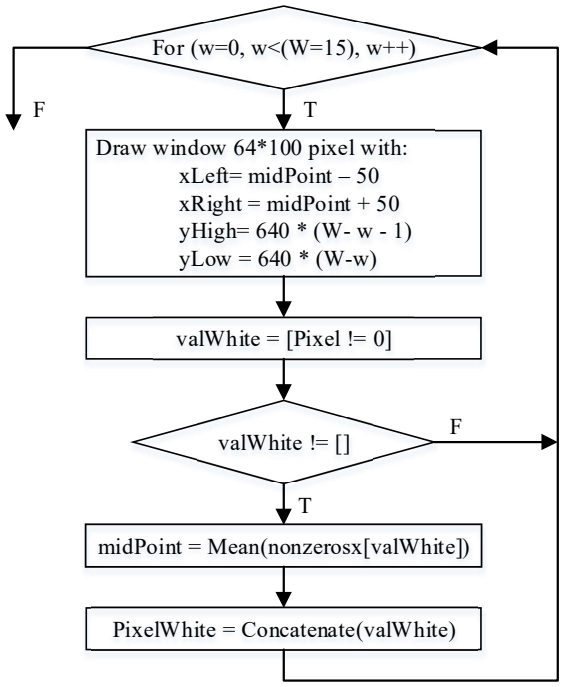

Figure 3: The sliding window protocol with the algorithm diagram

The welding seam will be accurately rebuilt by a quadratic polynomial regression model, as in Eq. (2):

$$CL = \beta_0 + \beta_1 . x + \beta_2 . x^2 \quad (2)$$

where x is a x coordinate of a center point of a moving window. The values β_i are determined by the numpy.polyfit() function for the (x, y) coordinates of the zero pixels, while ε is a small Gaussian noise with a zero mean, and from there extract the contour. The results are as shown in Figure 2.e.

2.1.3. *Calculating the angle deviation*

After drawing the contour on the real image as shown in Figure 2.f, we use the cv2.minAreaRect() function to calculate the deviation angle of the welding seam relative the vertical. The value of the deviation angle is processed by the method or formula to minimize the error, then sent to the central processing unit. The cv2.minAreaRect() function in the Open CV library introduced in [16] calculates the deflection angle of the robot relative the welding seam. The principle is as in Figure 4:

- If the height is greater than the width, the deflection angle is the angle between the contour and the horizontal;
- If the height is less than the width, the deflection angle is the angle between the contour and the vertical.

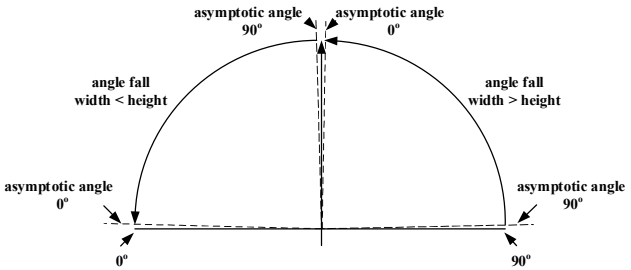

Figure 4: The angle values of the cv2.minAreaRect() function

Because the feedback deflection angle of this function is inconsistent with the calculation method and the robot controller, we need to convert it to the deviation angle value described in Figure 5.

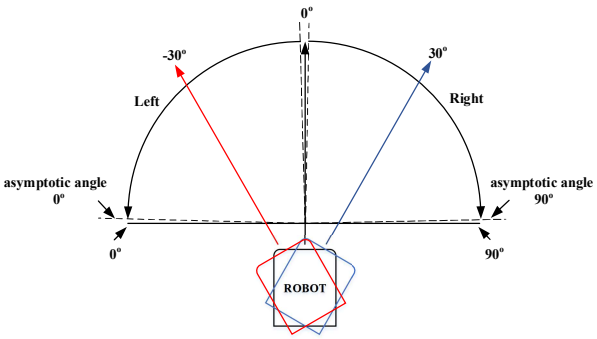

Figure 5: Deviation angle values

The conversion rule, as follows:

- If height > width then Ang = Ang – 90°;
- If height < width then Ang = Ang.

In the image processing, semiconductor cameras are often preferred over vacuum tube cameras. From the analyzed algorithms, the camera selected in this study must have the high quality, the low signal noise and the light sensitivity, lens from 18 to 108 *mm*. Moreover, it has the ability to white balance and adjust the image color automatically, minimum resolution 720 pixels, frame rate 30 fps.

2.2. Wheel traction and torque

Due to practical requirements, the welding inspection is usually performed on metal surfaces with an inclination from 0° to 180°, so in this study, we use the magnet wheels to help the robot cling and move on the metal surface with different inclinations.

The robot wheels are designed with the hard plastic drill holes alternately to attach magnets to stick to the steel surface. From the force analysis in Figure 6, let D denote the swing arm, while F_M as a magnet's attraction and the study also shows that the components of gravity play different roles when the robot moves on an inclined surface. Gravity component P_y works to keep the robot stationary on the surface, gravity component P_x pulls the robot downwards, as the drag force.

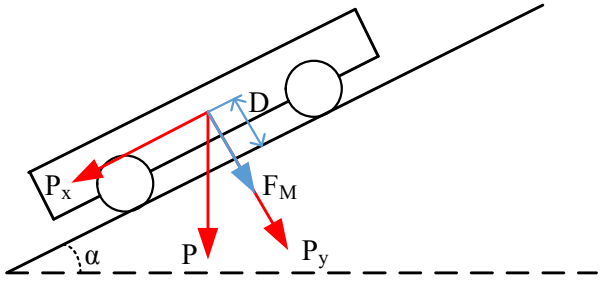

Figure 6: The force analysis of the robot with the plate angle α

At inclination angle, the "flip force" is the component of gravity P_y that opposes the movement of the robot, which tends to "pull" the robot down. "Flip force" is calculated according to the following formula:

$$F_{fall} = m.g.\cos(\alpha) \tag{3}$$

where m is the weight of the robot, g is the gravitational acceleration, and α is the angle of inclination of the steel plate.

At the same time, the component P_x of gravity and the friction force during the movement also cause the drag moment. This resistance changes when the angle of inclination changes, so it is necessary to calculate the load torque in each case to have an appropriate engine selection plan.

The components P_x of gravity, as in Eq. (4):

$$P_x = m.g.\sin(\alpha) \tag{4}$$

Besides, the robot still has the friction force F_{ms}, as in Eq. (5), with K is the frictional coefficient:

$$F_{ms} = m.g.\cos(\alpha).K \tag{5}$$

Thereby, the load torque total T_c is defined as in Table 1

According to the test results in Table 1, it shows the change of the "flip force" and the load torque when the tilt angle of the robot changes. The maximum "flip force" at 180° inclination with the value of 97 N, the maximum load torque is about 1.53 Nm when tilting the robot at an angle of 60°.

To ensure that the robot always sticks to and moves on metal surfaces with an inclination of up to 180°, the magnet's attraction must be greater than 97 N and the total torque of the four motors greater than 1.53 Nm. From that point, come up with a design plan for the magnet wheel and choose the appropriate motor.

Table 1: Flip force and load torque values of the robot

α (°)	F_{fall} (N)	T_c (Nm)
0	97	1.05
30	84	1.38
60	48	1.53
90	0	1.48
120	–48	1.23
150	–84	0.84
180	–97	0.43

Because the wheels are attached with magnets, they cannot absorb the vibration as well as rubber wheels. This will affect the ability to sample and the level of accuracy in image processing. However, we can replace with the gimbal to reduce the camera shake when moving. In additional, we can upgrade camera with high fps to increase sampling rate. sampling rate, which will make the image clearer.

2.3. Robot controller

2.3.1. *Differential transmission*

The concept of the differential transmission model consists of two independently driven wheels on a common axle. We can adjust the speed of each wheel to control the robot to move forward, backward, turn left, turn right [13]. When the robot moves on a curve whose temporary center is ICC, R is the distance between the wheels to the ICC, l is the distance between the centers of the wheels and V_l, V_r is the left, right wheel speed of the robot moving on that curve, while ω is the angular velocity. Speed calculation formula as follow:

$$\begin{cases} V_r = \omega.(R + l/2) \\ V_l = \omega.(R - l/2) \end{cases} \tag{7}$$

and

$$\begin{cases} R = \frac{1}{2}\left(\frac{V_r + V_l}{V_r + V_l}\right) \\ \omega = \frac{V_r + V_l}{l} \end{cases} \tag{8}$$

There are three cases for robots:

- Case 1: $V_l = V_r$ concludes that the robot moves in a straight line $R = \infty$ and $\omega = 0$;
- Case 2: $V_l = -V_r$ concludes that the robot rotates according to the point between the two wheel axes $R = 0$, and the robot rotates on a plane;
- Case 3: $V_l = 0$ or $V_r = 0$ concludes that the robot rotates in one direction $R = l/2$.

2.3.2. *Automatic Controller*

Due to the kinematics of the robot analyzed by the above formula, this study applies linear feedback control with PID controller to minimize the setting error and increase the response characteristic to ensure a stable system.
The general function of the PID controller:

$$F_R(s) = \frac{U(s)}{E(s)} = k_p + \frac{1}{\tau_I . s} + \tau_D . s \tag{9}$$

where s is the Laplace operator in the Laplace domain, while k_p, τ_I, and τ_D are all nonnegative, denote the coefficients for the proportional, integral, and derivative terms respectively.

To build the controller structure, the study proposes to use the two–loop cascade diagram including: deviation angle control and speed control presented as shown in Figure 7.

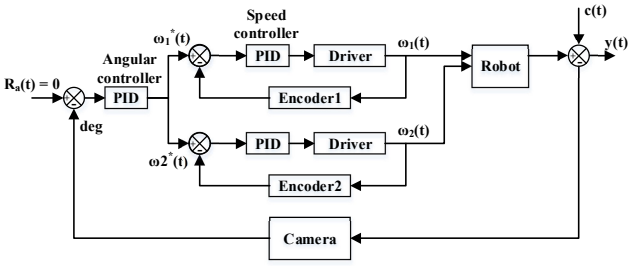

Figure 7: The controller structure

- Speed controller: Input value is set speed ω^*. The encoder speed sensor measures the current speed ω of the robot. Then the PID controller calculates the deviation and generates a signal to control the motor. Since the speed feedback is a scaler with a delay time τ_ω, and a proportional constant K_ω, it should be modeled as follows:

$$G_\omega(s) = \frac{K_\omega}{1 + \tau_\omega s} \tag{10}$$

The gain ratio of the selected speed feedback unit is 1 and the response time delay is ignored for easier calculation. This speed is compared with the set speed. The deviation will be sent to the PID controller to calculate the appropriate number of pulses in order to supply to the motor.

- Deviation angle controller: The input value is 0 and the feedback value is the offset angle value returned from the image processing module. The PID calculates the offset and gives the set speed ω^*. Since the two motors are independently controlled, a speed comparator is required to adjust the appropriate speed in each wheel, ensuring the deflection angle is approximately zero;

Based on the image processing technology, the deviation of the robot from the welding can be determined, and so the gain ratio of the selected feedback unit is 1. As a result, we simplify the module as follows:

$$G_\alpha(s) = \frac{2s}{1 + K_d s^2 + K_p s + K_i} \tag{11}$$

By using the module optimization method, the following coefficients can be calculated: Kp = 0.023, Ki = 0.0008, Kd = 0.018.

2.4. Experiment and estimate the results

2.4.1. *Experimental Results*

Complete the robot as designed and put it to the test in a real environment. Basic tests include:

- Testing the ability to recognize welding: When the robot runs about 15m, due to the cumulative error of the PID, the robot will detect the weld line with a difference of about 5 degrees compared to the actual weld;
- Testing the ability to adhere to metal surfaces with varying angles of inclination as shown in Figure 9;
- Testing robots operating in automatic and manual modes, monitoring parameters. Because of the limitation about device, the manual mode controlled by smart phone only operates normally with distance about 20 m.

The welding seam rebuilt from the actual image by the image edge detection algorithm and the sliding window protocol meets the requirements set forth. The calculated command angle has reliable accuracy.
The robot can grip and move on metal surfaces along the welding seam with inclinations from 0˚ to 180˚. The aluminum chassis is designed as in Figure 8, so it is light in weight and the wheels combined with the rotating axle help the car move flexibly on metal surfaces. The camera is placed in front, expanding the viewing angle, towards the development of applications to predict the direction of the robot in the future.

2.4.2. *Estimate the Results*

The robot's manufacturing and testing process has shown the following highlights:
• The robot recognizes and moves along the welding seam accurately in real time;

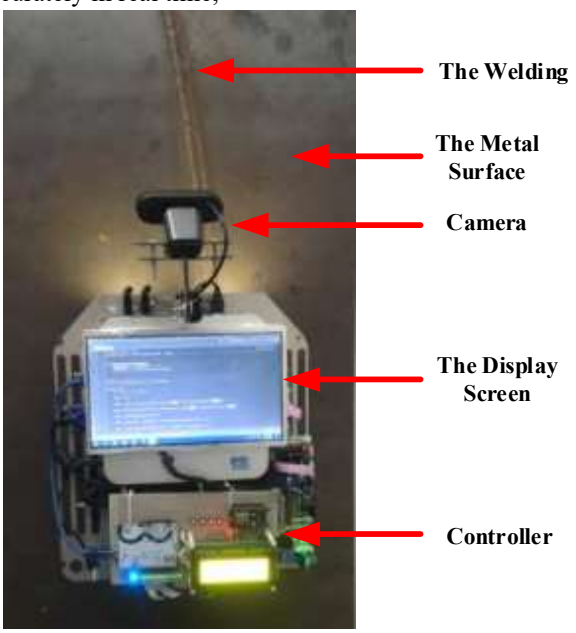

Figure 8: The structure of the robot

- The height, the width, and the weight of the robot are about 300 mm, 500 mm and 7 kg, the diameter and the thick of the wheels are 800 mm and 50 mm, from that, the maximum load weight of the robot is about 10 kg. This was tested in the real environment, so if the equipment is lighter than maximum weight, the robot definitely works as usual. However, with the heavy equipment, the speed is decreased and it is more dangerous. We can improve by replacing the motor with bigger moment and reinforced the robot's frame;
- Computational time of the whole system is based on processing and communication time. PC mini and microchip can implement with the frequency 10^6 to 10^8 Hz, so the authors can determine the computational time to be about 1 ms;
- Difference from detecting the welding metal by detecting different height between weld and surface with the CSL device made up of a cross laser projector, a CCD camera, and using the optical reflection principle [20], using the image processing is cheaper and simpler, it is also good at detecting the welding metal with the color's surface.

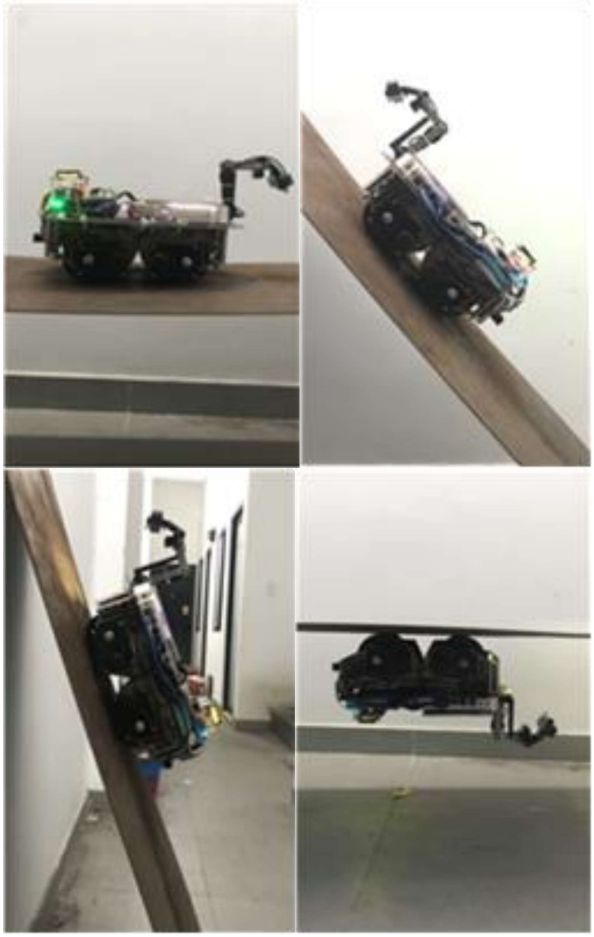

Figure 9: Testing the robot with different plate angles (0˚ , 45˚, 90˚, 180˚)

- The robot's ability to stick on metal surfaces is satisfactory and does not fall when the robot moves stably;
- Rugged chassis design, ensuring operation in outdoor environments.

However, robots still have limitations that need to be further researched and improved on the following points:

- The direction of light from the outside can affect the ability to analyze and process images. Therefore, falsifying the return parameters leads to incorrect operation of the robot;
- Using a magnet wheel increases surface friction when the robot works on a horizontal plane, wasting energy, reducing the robot's movement speed and flexibility;
- Image processing module can be affected by the outside light source. If the luminous intensity is so high, the robot is too difficult to detect the welding line because the metal surface reflects the strong light to camera.

3. Conclusions

In this study, image processing technology with Python's Open CV library is used and integrated into the robot's controller to enable real-time continuous welding detection based on recorded images. This proposal has practicality, high potential for developing and perfecting products, meeting the needs from reality. In many cases, the use of autonomous robot vehicles will reduce costs and time, reduce risks for technicians.

In the coming time, we will continue to research to improve the hardware as well as control solutions to limit the frictional force generated by the magnet wheels when the robot moves on a horizontal plane, improve control algorithm to reduce the impact of light noise the impact of light noise. In addition, we will continue to research and integrate more techniques to check the condition of equipment and steel structures to upgrade the function of the robot to serve the fault diagnosis to support the customers, condition-based maintenance planning for production facilities, wind power projects, pipeline systems, etc.

Acknowledgement

This work was supported by The Powermore Company Limited and The University of Danang, University of Science and Technology.

References

[1] S. W. Wen, P. Hilton, and D.C.J. Farrugia (2001), Finite element modelling of a submerged arc welding process. J. Materials Processing Technology, vol. 119, pp. 203–209.

[2] K. Lange (1997), Modern metal forming technology for industrial production. J. Materials Processing Technology, vol. 71, pp. 2–13.

[3] G. Caprari, A. Breitenmoser, W. Fischer, C. Hurzeler, and O. Nguyen (2012), Highly compact robots for inspection of power plants. J. Field Robotics, vol. 29, pp. 47–68.

[4] R. P. Feynman, R. B. Leighton, and M. Sands (1965), The Feynman lectures on physics. J. Phys. America, vol. 33, pp. 750–752.

[5] O. Kermorgant (2018), A magnetic climbing robot to perform autonomous welding in the shipbuilding industry. Robotics and Computer Integrated Manufacturing, vol. 53, pp. 178–186.

[6] T. H. Chung, G. Hollinger, and V. Isler (2011), Search and pursuit evasion in mobile robotics. Autonomous robots, vol. 31, pp. 299–316.

[7] D. Schmidt, and K. Berns (2013), Climbing robots for maintenance and inspections of vertical structures-A survey of design aspects and

[8] H. G. Lee, Y. S. Ryuh, W. H. Son, H. D. Jeong, and S. Park (2005), Design of a Mobile Robot System for Integrity Evaluation of Large Sized Industrial Facilities. J. Inst. Control, Robotics and Systems, vol. 11, pp. 595–601.

[9] W.O. Saxton, T. Pitt, and M. Horner (1979), Digital image processing: the Semper system. Ultramicroscopy, vol. 4, pp. 343–353.

[10] Issac, Ashish, M. Partha Sarathi, and Malay Kishore Dutta (2015), An adaptive threshold based image processing technique for improved glaucoma detection and classification, vol. 2, pp. 229-244

[11] Moon, S. W., Kim, Y. J., Myeong, H. J., Kim, C. S., Cha, N. J., & Kim, D. H (2011), Implementation of smartphone environment remote control and monitoring system for Android operating system-based robot platform, vol. 8, pp. 211-214

[12] R. J. Duan, Q. Li, and Y. Li (2005), Summary of image edge detection. Optical Technique, vol. 3, pp. 415–419.

[13] Q. Xiaowen (2011), Image processing based on openCV. Electronic Testing, vol. 7, pp. 39–41.

[14] X.Fengyu, S. Jingjin, and J. Guoping (2015), Kinematic and dynamic analysis of a cable climbing robot. Int. J. Advanced Robotic Systems, vol. 12, pp. 99.

[15] technologies. Robotics and Autonomous Systems, vol. 61, pp. 1288-1305.

[16] N. Pinckey (2006), Pulse width modulation for microcontroller servo control. IEEE Potentials, vol. 25, pp. 27–29.

[17] J. Singla, and R. Goyal (2012), A systematic way of affine transformation using image registration. Int. J. Information Technology, vol. 5, pp 239–243.

[18] Y. Meng, C. Jiang, H. Chen, and Y. Ren (2017), Cooperative device to device communications: Social networking perspectives. IEEE Networking, vol. 31, pp. 38–44.

[19] A. Rosenfeld (1969), Picture processing by computer. ACM Computing Surveys, vol. 1, pp. 147–176.

[20] L. Zhang, Q. Ye, W. Yang and J. Jiao (2014), Weld Line Detection and Tracking via Spatial-Temporal Cascaded Hidden Markov Models and Cross Structured Light. IEEE, vol. 63, pp. 120-140.